http://eprints.gla.ac.uk/64863

Deposited on: 02 September 2013

The dynamic crossover in water does not require bulk water

David A. Turton[a,c], Carmelo Corsaro[b], David F. Martin[c], Francesco Mallamace[b] and Klaas Wynne[a]
[a]School of Chemistry and WestCHEM, University of Glasgow, Glasgow, G12 8QQ, UK
[b]Dipartimento di Fisica and Consorzio, Nazionale Interuniversitario per le Scienze Fisiche della Materia, Università di Messina, I-98166 Messina, Italy
[c]Department of Physics, SUPA, University of Strathclyde, Glasgow G4 0NG, UK

Abstract

Many of the anomalous properties of water may be explained by invoking a second critical point that terminates the coexistence line between the low- and high-density amorphous states in the liquid. Direct experimental evidence of this point, and the associated polyamorphic liquid-liquid transition, is elusive as it is necessary for liquid water to be cooled below its homogeneous-nucleation temperature. To avoid crystallization, water in the eutectic LiCl solution has been studied but then it is generally considered that "bulk" water cannot be present. However, recent computational and experimental studies observe cooperative hydration in which case it is possible that sufficient hydrogen-bonded water is present for the essential characteristics of water to be preserved. For femtosecond optical Kerr-effect and nuclear magnetic resonance measurements, we observe in each case a fractional Stokes-Einstein relation with evidence of the dynamic crossover appearing near 220 K and 250 K respectively. Spectra obtained in the glass state also confirm the complex nature of the hydrogen-bonding modes reported for neat room-temperature water and support predictions of anomalous diffusion due to "worm-hole" structure.

Introduction

The solubility of LiCl in water is exceptionally high and because the eutectic solution (6.76 M) can be cooled into the glass, it is possible to study water (in solution) at temperatures where crystallization would occur in neat water. According to the Hofmeister series, both the lithium and chloride ions have a relatively weak influence on the structure of water (at low concentration) but the (high-charge density) Li ion forms a stable first solvation shell of water molecules and the general view is that at the eutectic concentration (where there are just seven water molecules per ion pair) no bulk water remains. Nevertheless, Mishima has proposed that the phase behaviour of aqueous LiCl solution is closely linked to that of water[1] and recent studies of the behaviour of the eutectic solution at low temperatures match the predictions of a dynamic crossover in neat water that would occur if the homogeneous nucleation temperature could be crossed.

Recent simulations have shown that water bridging, between the anions and cations, and ion cooperativity play a significant role in the hydration of ions.[2] These effects will reduce the number of water molecules necessary for ion hydration and suggest that even in concentrated solution, there is a possibility of residual bulk water, i.e. water "nanopools", in which the essential properties of bulk water might persist. Experiments employing infrared absorption spectroscopies[3] now suggest that cooperative hydration is indeed characteristic of salt solutions. Since salt solutions can be kept at atmospheric pressure they are arguably more similar to bulk water than nanoconfined systems and represent the closest experimental model system to neat water at low temperature. The above observations therefore warrant further study.
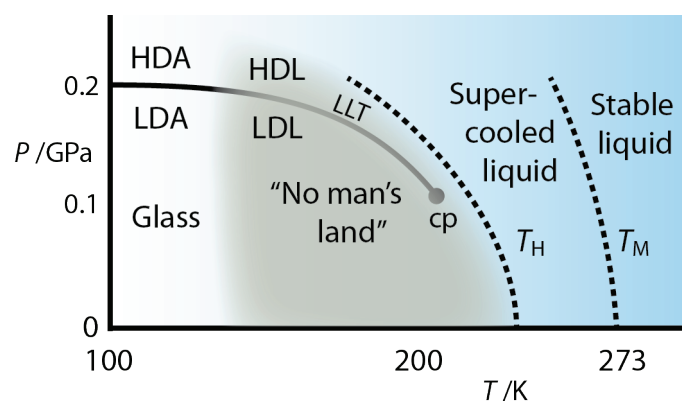
Fig. 1. *The phase diagram proposed by Mishima and Stanley[4] for the non-crystalline states of water shows the putative second critical point **cp** that lies in the experimentally inaccessible region below the homogeneous nucleation temperature T_H. The liquid-liquid transition associated with this point arises from the observed transition between the high and low density amorphous phases.*

Many of the curious properties of water that arise from the strong directional hydrogen bonding become more pronounced as it is supercooled towards a singular temperature where the thermodynamic properties appear to diverge.[5-8] Following the observation of a pressure-induced first-order phase change in the glassy state,[9] molecular dynamics simulations[10] suggested that there should be a second critical point terminating a coexistence line between the low- and high-density amorphous phases (Fig. 1).[4,11-17] The continuation of this line into the supercooled liquid state constitutes a liquid-liquid transition (LLT) and this has been proposed as a mechanism for the anomalous temperature dependence of the transport properties. Close to the glass transition the temperature dependence is Arrhenius-like "strong", while supercooled water is highly non-Arrhenius "fragile", and therefore a fragile to strong transition at *ca.* 230 K has also been proposed.[12] Although investigation of this region is hence crucial to understanding many of the essential characteristics of liquid water, direct experimental evidence is elusive as the putative second critical point and the associated LLT lie below the homogeneous nucleation temperature ($T_H \approx 238$ K), *i.e.*, in "no man's land" the region where bulk water will always crystallize spontaneously.[6,18]

Surprisingly, despite the expected absence of bulk water, investigation of LiCl solution has shown characteristics similar to these predictions: The temperature dependence of the hydrogen bonded structure in LiCl·6H$_2$O when studied by neutron scattering showed a dynamic crossover at *ca.* 210 K.[19,20] Employing nanopores in which confined liquid water can be cooled to near the glass transition temperature, nuclear magnetic resonance (NMR) and quasi-elastic neutron scattering data suggested evidence of the dynamic crossover as a breakdown in the Stokes-Einstein coupling of the microscopic and macroscopic transport dynamics.[21,22] Further evidence, in nanoconfined water, of the fragile-to-strong transition, second critical point, and LLT was obtained by infrared spectroscopy.[23] Mishima also observed a polyamorphic phase change in the glassy state of LiCl solution similar to that of water and again indicative of the LLT,[17,24] while recently Mamontov and co-workers measured a dynamic crossover in concentrated aqueous solutions of LiCl at 220 to 225 K.[25,26]

This puzzling situation might be explained by recent large-scale molecular dynamics simulations of moderate concentration LiCl solution in which the liquid-liquid transition is very much present.[27] In neat water, the transition to low density liquid water arises from an increase in the degree of hydrogen bonding to give water that is ice-like (It has been proposed that it is the LDL water formation step that results in homogeneous nucleation for the neat liquid). The same process occurring in salt solution drastically reduces the solubility of the salt (the solubility of salt in ice is very low) so as LDL water forms, the salt is expelled and the liquid decomposes into nanoscale regions of LDL water surrounded by high concentration brine.

Here, using optical Kerr-effect (OKE) spectroscopy, we first address the question of whether the eutectic solution can be seen as a reasonable analogue for neat water. We then probe the diffusional dynamics of the solution by both OKE and pulsed field-gradient NMR and demonstrate that, in each case, the effects of the dynamic crossover are evident.

Methods

Samples were prepared using anhydrous LiCl (>99%), deionized water, and D$_2$O (99.99%, all Sigma-Aldrich). A stock solution of LiCl in water was prepared at a concentration of 13.24 M determined by titration using Mohr's method. This was diluted volumetrically to give the eutectic concentration (6.76 M)[28]. This corresponds to a

solution of water with 25 mass% LiCl, 7.86 mol/kg, and 7 water molecules per LiCl. The solubility of LiCl in water is >35 mol% at 273 K. All samples were degassed before the measurements.

The ultrafast optical Kerr-effect (OKE) experiment measures the reduced Raman spectrum in the time domain. To measure the weak signal from water over a great enough range to capture the relaxational decay two OKE set-ups were employed. The faster dynamics were measured using a 7 nJ 20 fs pulse laser oscillator as described previously,[29] while a similar set-up employing a regeneratively-amplified laser (Coherent Legend USX) with a 1 μJ pulse stretched to a duration of *ca.* 1 ps was used to increase the signal-to-noise of the weaker relaxation measured at longer times. The two measured time-domain signals could be overlapped by greater than an order of magnitude in time allowing accurate concatenation.[30] The liquids were contained in a fused-quartz cuvette with a path length of 2 mm and the temperature was controlled by a cryostat (Oxford Instruments, Optistat DN, ±0.01 K). The frequency-domain OKE signal is derived from the time-domain measurement through a Fourier transform. This spectrum is deconvoluted from the instrument response, correcting for the finite spectral width of the laser pulse, by dividing by the Fourier transform of the autocorrelation of the laser pulse temporal profile.[31]

Complementary pulsed field gradient NMR diffusion measurements were performed that report on the macroscopic self-diffusion coefficient (DS) and the average translational relaxation time. A maximum gradient amplitude of 50 G cm^{-1} was used with a gradient pulse duration from 1 to 7 ms, and diffusion time from 100 to 800 ms.

The bulk (shear) viscosity was measured on a Bohlin Gemini II rheometer with a single measurement over a range of 189 to 280 K and (for lower viscosities) on a Cambridge Viscosity ViscoLab 3000 from 230 to 325 K. As a convenient method of parameterization, the combined data were fitted by the Vogel Fulcher Tammann (VFT) expression $\eta = \eta_0 \exp\left(DT_0 / \left(T - T_0\right)\right)$. For viscosity η this model introduces a singular temperature T_0 where the dynamics are apparently arrested. The deviation from Arrhenius behaviour, also known as the fragility, is described by the parameter D. For the viscosity range measured here the fit gives $D \approx 4.1$ consistent with the typically high fragility of hydrogen bonding liquids.[32]

Results

The strong directional hydrogen-bonding interactions of water give rise to several distinct bands in the terahertz Raman spectrum and simulations have shown these to require a hydrogen-bonded tetrahedral water pentamer.[33] The reduced Raman spectrum can be measured with good sensitivity in this region by femtosecond optical Kerr-effect (OKE) spectroscopy.[34-37]

OKE spectroscopy measures the derivative of the polarizability-polarizability time-correlation function in the time domain and is sensitive to the square of the anisotropic part of the many-body polarizability tensor,

$$S_{OKE}(\tau) \propto \frac{1}{k_B T} \frac{d}{d\tau} \left\langle \ddot{\Pi}_{xy}(\tau) \ddot{\Pi}_{xy}(0) \right\rangle.$$

The OKE spectrum is given by the taking the Fourier transform and dividing this by the Fourier transform of the laser pulse (deconvolution) yielding the (Bose-Einstein population-corrected) depolarised Raman spectrum. The slowest components of this spectrum are normally assigned to rotational modes that report on structural relaxation. However, the polarizability tensor for water has a surprisingly low degree of anisotropy. Therefore the measurement is primarily sensitive to interactions (collisions) and hence to translational motion. In Fig. 2, the OKE spectrum for the eutectic solution of LiCl is compared to that of neat water. Below 400 cm^{-1} there are no intramolecular contributions and the spectrum consists of three main broad features. At lowest frequency is the relaxational mode that appears at ~10 cm^{-1} (300 GHz) in neat water at room temperature. On addition of salt, the viscosity increases and this mode shifts to lower frequency. We have previously shown that this behaviour in concentrated aqueous electrolyte solutions is consistent with the slowdown of translational motions due to the formation of nanopools of water.[35] At higher frequency, two bands are readily identified at *ca.* 60 cm^{-1} (1.8 THz) and 180 cm^{-1} (5.4 THz). In Raman studies of water, Walrafen assigned these bands as respectively the transverse acoustic (TA) and the longitudinal acoustic (LA) mode, *i.e.*, the short wavelength phonon modes observed at the Brillouin zone edge.[38,39] For convenience we use the TA and LA notation herein.
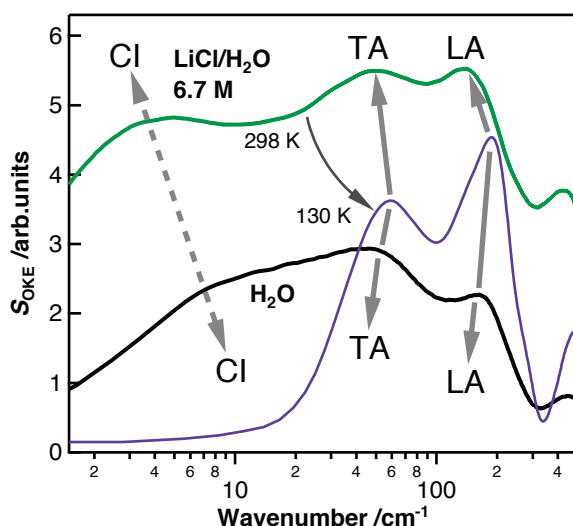
Fig. 2. *As the molecular polarizability tensor of water is very nearly isotropic, the reduced Raman (OKE) spectrum of neat water (black) is very weak and dominated by intermolecular modes. The spectrum of water in the salt solution at room temperature (green) is stronger due to the presence of the more polarizable anions. The relaxational mode (R) is strongly dependent upon temperature (frozen-out in the glass) and salt concentration.[35] The longitudinal (LA) and transverse acoustic (TA) hydrogen-bond modes[40] broaden and shift to lower frequency on addition of the salt but then narrow again at lower temperature (purple) indicating that the hydrogen-bonding structure recovers. The higher frequency modes above ca. 400 cm⁻¹ are due to intermolecular librational motions of the water molecule.*

The LA band at higher frequency is often associated more simply with the longitudinal stretch of a hydrogen-bonded O–O–O motif or of the canonical tetrahedrally hydrogen bonded "Walrafen pentamer".[40] The origin of the TA band has been more controversial,[33,41,42] but most often it is described similarly as a transverse motion (or bend) of the hydrogen bond. Molecular dynamics simulations of rotational dynamics of water[43] and recent simulations of supercooled bulk water at 180 K[44] find that the TA mode has mixed rototranslational origins while the LA mode is a doublet comprising the antisymmetric and symmetric stretch of the tetrahedrally-bonded pentamer.

On addition of the salt, no additional modes are evident. The lithium ion has a very low polarizability making the contributions due to its intrinsic motions relatively weak. The strength of the water-chloride ion bond is very similar to the water-water bond and it is known that the chloride ion is relatively benign with respect to the hydrogen bond structure. In contrast, the lithium ion forms a stable hydration shell in which water motions are constrained to small angle oscillations, i.e. librations, that are most likely to contribute at higher frequency in the part of the spectrum that is inaccessible here.

In the room-temperature eutectic solution, the TA and LA bands are broadened and shifted slightly to lower frequency consistent with a moderate disruption of hydrogen bonding by the ions. However, for similar solutions neutron scattering studies have suggested that on cooling the degree of hydrogen bonding again increases and the tetrahedral structure reforms.[20] In the OKE experiments, we cooled the eutectic solution to 130 K and at this temperature the TA and LA modes shift back to higher frequency and also strengthen indicating that the tetrahedral structure indeed reappears. This behaviour is also consistent with the results of recent neutron diffraction experiments on dilute LiCl solution that show that at low temperature the liquid appears more similar to low-density amorphous water, i.e., that the structure is expanded due to the increased degree of hydrogen bonding.[45]

In infrared absorption and Raman studies, the TA and LA bands appear to be relatively featureless but Winkler *et al.* recorded Raman spectra for neat water and showed that this region has complex structure.[46] At room temperature (Fig. 2), these bands are broad and the differences between neat water and LiCl solution are hard to quantify; even apparent changes in amplitude can be misleading since the relaxation mode is considerably overlapped. At lower temperatures however, the structure in the spectrum is better resolved and in Fig. 3 the spectrum of the eutectic solution at 130 K is shown. If a simple inhomogeneously broadened (Gaussian) lineshape is assumed, five modes are necessary to adequately fit the low-frequency spectrum (details in Appendix A, Table 1). As seen in Fig. 2, the TA mode at *ca.* 60 cm⁻¹ is relatively unperturbed by the presence of the salt (as it is insensitive to temperature in neat water). In Figure 7 of Reference [46] for neat water at 0° C it is shown that the LA band, appearing nominally at 180 cm⁻¹, is in fact complex. Here at 130 K the structure is still present and is even better defined as seen by the strong bands at *ca.* 130 and 280 cm⁻¹. In the molecular dynamics simulation of Reference [44], Fig. 4 corresponds to the supercooled state at 180 K and, using

a large scale TIP4P model, reproduces the band at *ca.* 60 cm⁻¹ (11.3 rad /ps) very closely with two additional bands at *ca.* 150 and *ca.* 250 cm⁻¹ (30 and 48 rad /ps) very similar in frequency and bandshape to those in Fig. 3.
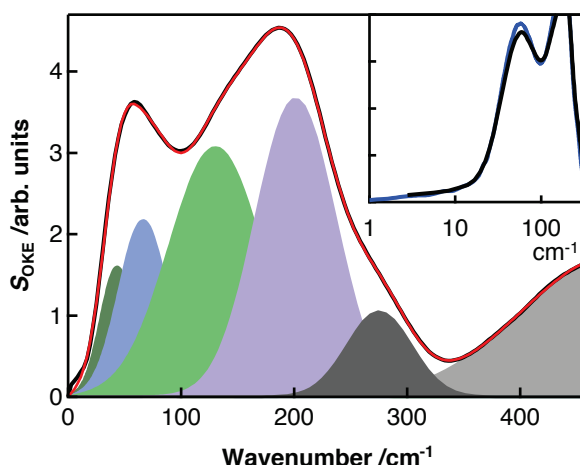

Fig. 3. *The reduced Raman (OKE) spectrum (linear frequency scale) for the eutectic solution of LiCl at 130 K (black) can be fit accurately by the sum of six Gaussian functions (red). Inset is detail (on a log frequency scale) showing the anomalous mode below 20 cm⁻¹ with the almost identical spectrum of LiCl in D_2O (blue). For details and fit parameters see (Appendix A).*

How can this strong similarity to bulk water be reconciled with the fact that the eutectic solution has only seven water molecules per ion pair? Experiments and simulations find a value for the first shell Li^+ hydration number of 3.5 to 4 at infinite dilution[47-49] while the Cl^- ion forms a weakly-bound shell of *ca.* six water molecules but has negligible impact on hydrogen bonding.[50] At the concentration of the eutectic solution there must inevitably be ion pairing and bridging of water molecules between ion pairs[3] that will reduce the number of water molecules necessary for hydration. Thus, a picture emerges of very small water pools containing upwards of one water-coordinated water molecule surrounded by water molecules weakly coordinating Cl^- (through the hydrogen atom) and more strongly coordinating Li^+ (through the oxygen atom). These small pools are large enough to support bulk-water behaviour and, although scattering studies measure a high degree of ion-water association, it appears that this water is still able to participate to a large degree in water–water hydrogen bonding. In fact, simulations show that the spectroscopically-sensitive dynamics of water are present in clusters as small as a single pentamer.[51]

Although calorimetric measurements for the eutectic solution show that at 130 K relaxation should be arrested, a relaxation is clearly observable, in the inset of Fig. 3, below 20 cm⁻¹ (corresponding to a timescale of several picoseconds). This motion is consistent between H_2O and D_2O. It is too extended to be the wing of a Gaussian-like band and so is most likely to be associated with the anomalous diffusion of the percolating ion-water network, for example, the "worm-hole" structure suggested by Angell *et al.*[52] or the "activated hopping process" through which nominally-arrested molecules in the glassy state can escape the cage structure.[53]

For the deuterated solution, very little difference is seen in the region below 300 cm⁻¹ since the slight red shift, due to the 10% increase in molecular mass, is small compared to the band widths. This does imply that the spectrum does not contain any significant combination bands and therefore that all the identified modes are intermolecular in origin.

Diffusional dynamics

The time-domain OKE signal for the eutectic solution of LiCl in water is shown over the range from room temperature to the glassy state in Fig. 4 where after *ca.* 1 ps the signal is dominated by the diffusional relaxation. The water molecule has a near-spherical polarizability so rotational modes are very weak and the measured signal is dominated by collision-induced translational motions.[35] The final diffusional decay is dissimilar to a simple Debye (exponential) decay and it has been shown that the dynamics are well described by (the time derivative of) the stretched exponential (Kohlrausch-Williams-Watts) function,[54], $S(t) \propto \frac{d}{dt} \exp\left(-(t/\tau)^\beta\right), 0 < \beta < 1$. For $\beta = 1$ the function corresponds to a simple exponential decay, i.e. a Debye function in the frequency domain.
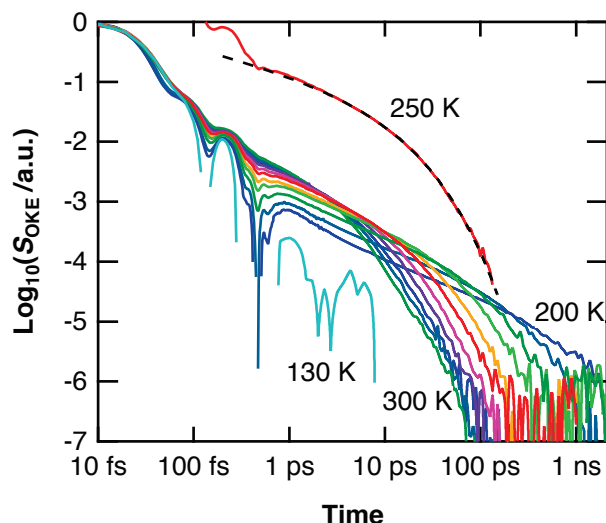
Fig. 4. *For the eutectic solution of LiCl in water, OKE spectroscopy allows the measurement of the dynamics over around five orders of magnitude (in time and amplitude) from 300 K to 200 K and in the glassy state at 130 K. The 250 K signal is also shown vertically offset with the (stretched exponential) fit (dashed curve) showing the quality of fit over four orders of magnitude in amplitude.*

The stretched exponential is consistent with the predictions of Mode-Coupling theory, and in this framework (of dynamics in the supercooled region) the stretching parameter β can be interpreted as a measure of structural heterogeneity. This function proved here also to be an effective model of the relaxation in the eutectic solution (Fig. 4). At temperatures above *ca.* 230 K the stretching parameter is reasonably constant and similar to that measured in neat water ($\beta \approx 0.6$), but in the region associated with the LLT drops sharply indicating a structural transition, Fig. 5.
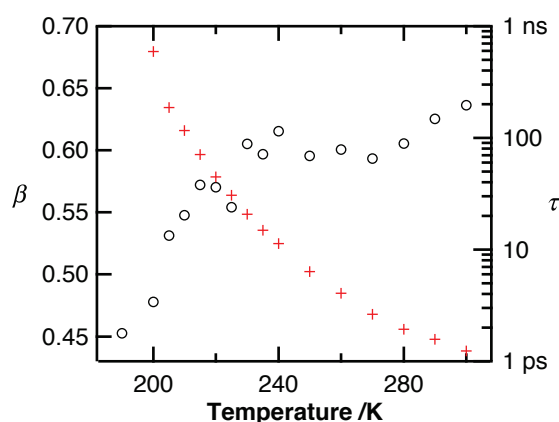

Fig. 5. *The parameters for the fit of the stretched exponential to the OKE data for the eutectic solution of LiCl in water over the range of temperature from 300 K to 190 K. The time constant τ (crosses) shows no sharp discontinuity but here the dynamic crossover is evident from the sudden increase in broadening through the stretching parameter β (circles) at 230 – 240 K.*

Over the measured temperature range, the liquid is *fragile* in that the curvature of the temperature dependence of the time constant is greater than can be reproduced by the Arrhenius equation (as would be the case for simple diffusion).[32] This is also true for viscosity, but although the viscosity can be fit by the Vogel-Fulcher-Tammann expression the curvature in the OKE time constant is more extreme. Single molecule diffusivity can be related to bulk viscosity in simple systems through the Stokes-Einstein relation, $D \propto (\eta/T)^{-1}$. Here a fractional Stokes-Einstein dependence[22] $D \propto (\eta/T)^{-\zeta}$ is observed (Fig. 6) as is the case for neat water.

Translational diffusion rates were also measured by NMR and are shown in Fig. 6. With respect to bulk viscosity, the NMR data are in close agreement with Stokes-Einstein behaviour at high temperatures with $\zeta \approx 1$, but the dynamic crossover is again apparent as ζ falls to *ca.* 0.8 although here, the crossover temperature is apparently higher at *ca.* 250 K. The OKE data also exhibit fractional Stokes-Einstein behaviour but, in contrast, $\zeta \approx 0.9$ over the whole temperature range. A disparity between the two techniques is to be expected as the NMR measurement is sensitive to long scale and hence average diffusional rates while the OKE measurement is

sensitive to nearest neighbour (very short scale) fluctuations through which the heterogeneity can be observed.
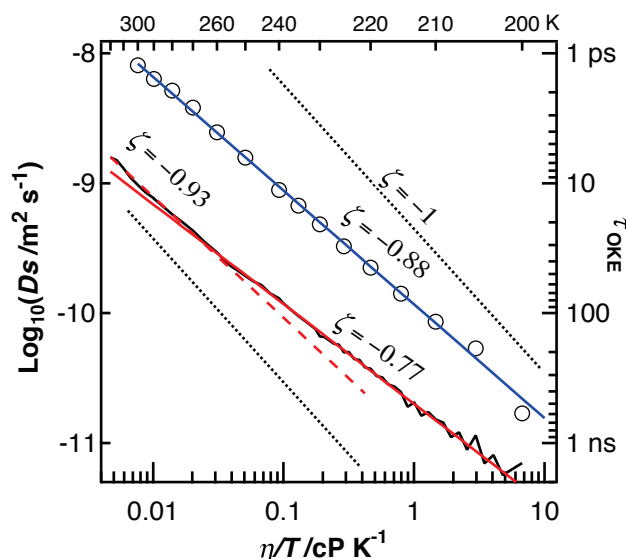

Fig. 6. *Both OKE (circles) and NMR (black line) time constants show fractional Stokes-Einstein behaviour when plotted against viscosity. However, while the OKE data can be fitted by a constant exponent of 0.88, the NMR data break at around 250 K. Normal Stokes-Einstein behaviour is indicated by the dotted lines.*

Discussion

As recently reviewed,[48,49] simulations differ as to the effect of solvated ions on the structure of water but are generally interpreted to mean that above moderate concentration little or no bulk water remains. Molecular dynamics simulations find that the residence times and dynamics of water in water–water and water–Cl⁻ hydration shells are very similar,[50] implying that the presence of the Cl⁻ ion has little influence on the extended hydrogen bond network. However, there is no doubt that the small Li cation forms a strongly bound hydration shell immobilizing water molecules and disrupting the tetrahedral structure of the bulk water. Scattering experiments reach similar conclusions and it has been suggested that the addition of salt decreases the number of hydrogen bonds in water similar to the effect of increasing pressure,[55,56] while time-of-flight neutron scattering measurements[57] observed that in ~8.3 M LiCl solution the number of hydrogen bonds falls to ~20% implying the complete disappearance of bulk water.

Nevertheless, the OKE spectra for neat water and the aqueous solutions of LiCl show many common features with the complex structure of the LA mode at *ca.* 180 cm⁻¹, which appears in both experiment and molecular dynamics simulations of bulk water and is strongly associated with the extended hydrogen bonding, still strongly in evidence. Taking into account ion bridging and cooperative hydration, the simple numerical estimates of free water in solution are misleading. The simplest explanation then is the presence of water nanopools containing upwards of a single water molecule that, through tetrahedral coordination to the surrounding water, is still able to reproduce the dynamics of bulk water. A residual "relaxational" mode is seen in the glass at 130 K, implying that these water pools are able to sustain a diffusive transport process. Similar structuring has been identified in mixtures of water with simple alcohols,[58] and the OKE data support previous observations that the tetrahedral hydrogen-bonding structure of water further recovers at low temperatures. These observations do not rule out the decomposition into low density water and brine, as previously suggested,[27] but, as the sharpening of the spectrum at low temperature is gradual, the liquid-liquid transition is not an abrupt one.

These observations may be relevant to studies of protein hydration water in which it has been suggested that a dynamic crossover is present.[59-61] In some cases, the agreement in temperature between this crossover and that predicted for neat water has led to the suggestion that it is the crossover in water that is driving the protein dynamics.[59] However protein hydration water is in a highly heterogeneous environment in which the behaviour of water is expected to be strongly modified and this is a vigorously debated area.[62-64]

Whatever there precise origin, the water nanopools in concentrated LiCl solution apparently contain sufficient associating water molecules for the low-temperature dynamic crossover to be detected by neutron-scattering experiments. Here, in OKE and NMR measurements of diffusion, there is again evidence of a dynamic crossover. In the NMR measurement this can be associated with the formation of increasing scale

heterogeneity, *i.e.* the diffusion of clusters that increase in size as the glass state is approached where the crossover reflects a change in distribution of the heterogeneity. The marked increase in heterogeneity observed in the OKE measurement reflects the same process but while the NMR observable is sensitive to the averaged diffusional motion the (collision-induced) OKE signal is sensitive to molecular-scale diffusion, such as cage breakup in the solvent-cage model, revealing subtly different dynamics that result in the difference in observed temperature.

Appendix A. Optical Kerr-effect analysis.

The fit to the OKE spectra for the eutectic solutions in water and D_2O, use a Gaussian function as a simple characteristic lineshape. For use at low frequencies the negative part of the spectrum must be included in order that the function is antisymmetric about zero frequency and hence obeys causality. Then, where A is the amplitude, ω_o is the resonance frequency, and γ is the rate of damping. This is commonly referred to as an *assymetrised* Gaussian.

$$S_G(\omega) = A\exp\left[-\frac{(\omega-\omega_0)^2}{2\gamma^2}\right] - A\exp\left[-\frac{(\omega+\omega_0)^2}{2\gamma^2}\right]$$

Table 1. Parameters for the six-Gaussian fit to 6.7 M H_2O/LiCl at 130 K and LiCl/D_2O at 125 K.

LiCl/H_2O						
	G_1	G_2	G_3	G_4	G_5	G_6*
A /a.u.	12	16	23	27	8	6
ω_o /cm^{-1}	43	66	130	201	275	460
γ /cm^{-1}	14	21	41	35	28	78
LiCl/D_2O						
	G_1	G_2	G_3	G_4	G_5	G_6*
A /a.u.	11	18	26	22	7	4
ω_o /cm^{-1}	43	64	143	203	266	360
γ /cm^{-1}	13	21	47	31	21	59

*The band above ~300 cm^{-1} comprises the three librational modes that are not resolved in the Raman spectrum.

1   O. Mishima, *J. Chem. Phys.*, 2005, **123**, 154506.
2   L. Petit, R. Vuilleumier, P. Maldivi and C. Adamo, *J. Chem. Theory Comput.*, 2008, **4**, 1040-1048.
3   K. J. Tielrooij, N. Garcia-Araez, M. Bonn and H. J. Bakker, *Science*, 2010, **328**, 1006-1009.
4   H. E. Stanley, S. V. Buldyrev, M. Canpolat, O. Mishima, M. R. Sadr-Lahijany, A. Scala and F. W. Starr, *PCCP*, 2000, **2**, 1551-1558.
5   H. E. Stanley and J. Teixeira, *J. Chem. Phys.*, 1980, **73**, 3404-3422.
6   C. A. Angell, *Annu. Rev. Phys. Chem.*, 1983, **34**, 593-630.
7   A. P. Sokolov, J. Hurst and D. Quitmann, *Phys. Rev. B*, 1995, **51**, 12865-12868.
8   F. Mallamace, C. Branca, C. Corsaro, N. Leone, J. Spooren, H. E. Stanley and S.-H. Chen, *J. Phys. Chem. B*, 2010, **114**, 1870-1878.
9   O. Mishima, L. D. Calvert and E. Whalley, *Nature*, 1985, **314**, 76-78.
10   P. H. Poole, F. Sciortino, U. Essmann and H. E. Stanley, *Nature*, 1992, **360**, 324-328.
11   O. Mishima and H. E. Stanley, *Nature*, 1998, **396**, 329-335.
12   K. Ito, C. T. Moynihan and C. A. Angell, *Nature*, 1999, **398**, 492-495.
13   L. M. Xu, P. Kumar, S. V. Buldyrev, S. H. Chen, P. H. Poole, F. Sciortino and H. E. Stanley, *Proc. Natl. Acad. Sci. U. S. A.*, 2005, **102**, 16558-16562.
14   P. Kumar, Z. Yan, L. Xu, M. G. Mazza, S. V. Buldyrev, S. H. Chen, S. Sastry and H. E. Stanley, *Phys. Rev. Lett.*, 2006, **97**, 177802.
15   C. A. Angell, *Science*, 2008, **319**, 582-587.
16   D. Banerjee, S. N. Bhat, S. V. Bhat and D. Leporini, *Proc. Natl. Acad. Sci. U. S. A.*, 2009, **106**, 11448-11453.
17   O. Mishima, *Proc. Jpn. Acad. Ser. B-Phys. Biol. Sci.*, 2010, **86**, 165-175.
18   P. G. Debenedetti and H. E. Stanley, *Phys. Today*, 2003, **56**, 40-46.

19   B. Prevel, J. Dupuyphilon, J. F. Jal, J. F. Legrand and P. Chieux, *J. Phys. Cond. Mat.*, 1994, **6**, 1279-1290.

20   B. Prevel, J. F. Jal, J. Dupuyphilon and A. K. Soper, *J. Chem. Phys.*, 1995, **103**, 1886-1896.

21   S. H. Chen, F. Mallamace, C. Y. Mou, M. Broccio, C. Corsaro, A. Faraone and L. Liu, *Proc. Natl. Acad. Sci. U. S. A.*, 2006, **103**, 12974-12978.

22   L. Xu, F. Mallamace, Z. Yan, F. W. Starr, S. V. Buldyrev and H. E. Stanley, *Nat. Phys.*, 2009, **5**, 565-569.

23   F. Mallamace, M. Broccio, C. Corsaro, A. Faraone, D. Majolino, V. Venuti, L. Liu, C. Y. Mou and S. H. Chen, *Proc. Natl. Acad. Sci. U. S. A.*, 2007, **104**, 424-428.

24   O. Mishima, *J. Chem. Phys.*, 2007, **126**, 244507.

25   E. Mamontov, *J. Phys. Chem. B*, 2009, **113**, 14073-14078.

26   E. Mamontov, A. Faraone, E. W. Hagaman, K. S. Han and E. Fratini, *J. Phys. Chem. B*, 2010, **114**, 16737-16743.

27   L. Le and V. Molinero, *J. Phys. Chem. A*, 2011, **115**, 5900-5907.

28   C. Monnin, M. Dubois, N. Papaiconomou and J. P. Simonin, *J. Chem. Eng. Data*, 2002, **47**, 1331-1336.

29   D. A. Turton, D. F. Martin and K. Wynne, *PCCP*, 2010, **12**, 4191-4200.

30   D. A. Turton, C. Corsaro, M. Candelaresi, A. Brownlie, K. R. Seddon, F. Mallamace and K. Wynne, *Faraday Discuss.*, 2011, **150**, 493-504.

31   D. McMorrow and W. T. Lotshaw, *Chem. Phys. Lett.*, 1990, **174**, 85-94.

32   C. A. Angell, *Chem. Rev.*, 2002, **102**, 2627-2649.

33   K. H. Tsai and T. M. Wu, *Chem. Phys. Lett.*, 2006, **417**, 389-394.

34   G. Giraud and K. Wynne, *J. Chem. Phys.*, 2003, **119**, 11753-11764.

35   D. A. Turton, J. Hunger, G. Hefter, R. Buchner and K. Wynne, *J. Chem. Phys.*, 2008, **128**, 161102.

36   D. A. Turton, J. Hunger, A. Stoppa, G. Hefter, A. Thoman, M. Walther, R. Buchner and K. Wynne, *J. Am. Chem. Soc*, 2009, **131**, 11140-11146.

37   D. A. Turton and K. Wynne, *J. Chem. Phys.*, 2009, **131**, 201101.

38   G. E. Walrafen, *J. Phys. Chem.*, 1990, **94**, 2237-2239.

39   G. E. Walrafen, Y. C. Chu and G. J. Piermarini, *J. Phys. Chem.*, 1996, **100**, 10363-10372.

40   G. E. Walrafen, *J. Chem. Phys.*, 1964, **40**, 3249-3256.

41   J. A. Padro and J. Marti, *J. Chem. Phys.*, 2003, **118**, 452-453.

42   A. de Santis, A. Ercoli and D. Rocca, *J. Chem. Phys.*, 2004, **120**, 1657-1658.

43   I. M. Svishchev and P. G. Kusalik, *J. Chem. Soc.-Faraday Trans.*, 1994, **90**, 1405-1409.

44   P. Jedlovszky, G. Garberoglio and R. Vallauri, *J. Phys.-Condes. Matter*, 2010, **22**, 284105.

45   K. Winkel, M. Seidl, T. Loerting, L. E. Bove, S. Imberti, V. Molinero, F. Bruni, R. Mancinelli and M. A. Ricci, *J. Chem. Phys.*, 2011, **134**, 024515.

46   K. Winkler, J. Lindner and P. Vöhringer, *PCCP*, 2002, **4**, 2144-2155.

47   W. Wachter, S. Fernandez, R. Buchner and G. Hefter, *J. Phys. Chem. B*, 2007, **111**, 9010-9017.

48   A. V. Egorov, A. V. Komolkin, V. I. Chizhik, P. V. Yushmanov, A. P. Lyubartsev and A. Laaksonen, *J. Phys. Chem. B*, 2003, **107**, 3234-3242.

49   Y. Marcus, *Chem. Rev.*, 2009, **109**, 1346-1370.

50   D. Laage and J. T. Hynes, *J. Phys. Chem. B*, 2008, **112**, 7697-7701.

51   W. B. Bosma, L. E. Fried and S. Mukamel, *J. Chem. Phys.*, 1993, **98**, 4413-4421.

52   C. A. Angell and R. D. Bressel, *J. Phys. Chem.*, 1972, **76**, 3244-3253.

53   S. H. Chong, *Phys. Rev. E*, 2008, **78**, 041501.

54   R. Torre, P. Bartolini and R. Righini, *Nature*, 2004, **428**, 296-299.

55   A. Botti, F. Bruni, S. Imberti, M. A. Ricci and A. K. Soper, *J. Chem. Phys.*, 2004, **120**, 10154-10162.

56   M. Kobayashi and H. Tanaka, *Phys. Rev. Lett.*, 2011, **106**, 125703.

57   R. H. Tromp, G. W. Neilson and A. K. Soper, *J. Chem. Phys.*, 1992, **96**, 8460-8469.

58   S. Dixit, J. Crain, W. C. K. Poon, J. L. Finney and A. K. Soper, *Nature*, 2002, **416**, 829-832.

59   S. H. Chen, L. Liu, E. Fratini, P. Baglioni, A. Faraone and E. Mamontov, *Proc. Natl. Acad. Sci. U. S. A.*, 2006, **103**, 9012-9016.

60   P. Kumar, G. Franzese and H. E. Stanley, *Phys. Rev. Lett.*, 2008, **100**, 105701.

61   M. G. Mazza, K. Stokely, S. E. Pagnotta, F. Bruni, H. E. Stanley and G. Franzese, *Proc. Natl. Acad. Sci. U. S. A.*, 2011, **108**, 19873-19878.

62   J. Swenson, H. Jansson and R. Bergman, *Phys. Rev. Lett.*, 2006, **96**, 247802.

63   S. Pawlus, S. Khodadadi and A. P. Sokolov, *Phys. Rev. Lett.*, 2008, **100**, 108103.

64   W. Doster, S. Busch, A. M. Gaspar, M. S. Appavou, J. Wuttke and H. Scheer, *Phys. Rev. Lett.*, 2010, **104**, 098101.

Supporting Information

Turton et al.
The dynamic crossover in water does not require bulk water

1. Optical Kerr-effect analysis

Table 2. Parameters for the six-Gaussian fit to 6.7 M H_2O/LiCl at 130 K and LiCl/D_2O at 125 K.

LiCl/H_2O

	G_1	G_2	G_3	G_4	G_5	G_6*
A /a.u.	12	16	23	27	8	6
ω_0 /cm^{-1}	43	66	130	201	275	460
γ /cm^{-1}	14	21	41	35	28	78

LiCl/D_2O

	G_1	G_2	G_3	G_4	G_5	G_6*
A /a.u.	11	18	26	22	7	4
ω_0 /cm^{-1}	43	64	143	203	266	360
γ /cm^{-1}	13	21	47	31	21	59

*For these liquids the spectra are unreliable above ~300 cm^{-1}.

The fit to the OKE spectra for the eutectic solutions in water and D_2O, use a Gaussian function as a simple characteristic lineshape. For use at low frequencies the negative part of the spectrum must be included in order that the function obeys causality, hence

$$S_{\mathrm{G}}(\omega) = A\exp\left[-\frac{(\omega-\omega_0)^2}{2\gamma^2}\right] - A\exp\left[-\frac{(\omega+\omega_0)^2}{2\gamma^2}\right] \tag{1.1}$$

where A is the amplitude, ω_o is the resonance frequency, and γ is the rate of damping. This is often referred to as an assymetrised Gaussian as it is antisymmetric about zero frequency.

The relaxational contribution to the spectrum was fitted by the stretched exponential (Kohlrausch-Williams-Watts) function,[1] $S(t) \propto \frac{d}{d\tau}\exp\left(-(t/\tau)^\beta\right), 0 < \beta < 1$. For $\beta = 1$ the function corresponds to a simple exponential decay, i.e. a Debye function in the frequency domain. In Figure S1 Fig. 7the stretched exponential function is compared to the Debye, Cole-Cole, and Cole-Davidson functions.[2]
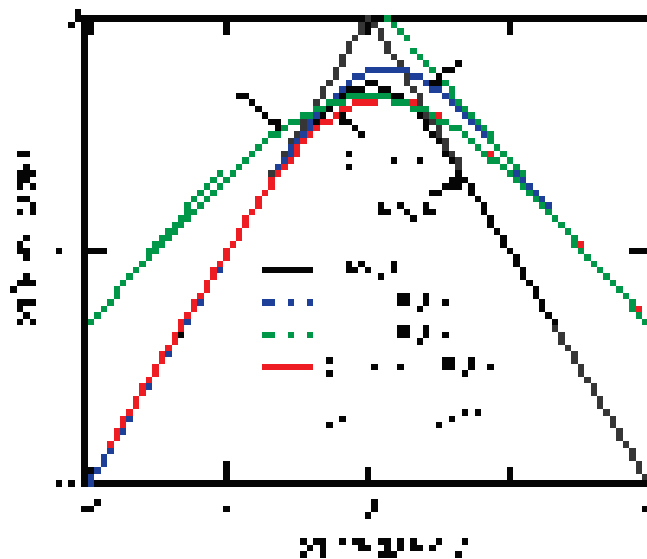

Fig. 7. *The stretched exponential function compared, as a function of normalized frequency, to the Debye, Cole-Cole (CC), and Cole-Davidson (CD) functions. The low frequency asymptote shows that the stretched exponential becomes Debye-like for long times.*
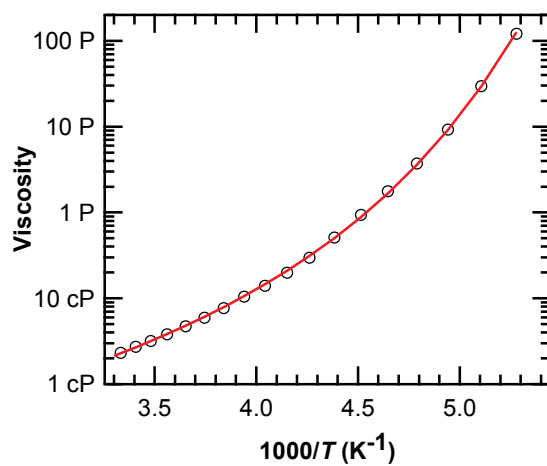
2. Viscosity measurements

Fig. 8. *The shear viscosity measured in 6.7 M H₂O/LiCl fit by the VFT function over the temperature range of 190 – 326 K.*

(1)   Torre, R.; Bartolini, P.; Righini, R. *Nature* **2004**, *428*, 296-299.
(2)   Havriliak, S.; Havriliak, S. J. *Polymer* **1996**, *37*, 4107-4110.